Highly Variable π-Bonding in the Interaction of Iron(II) Porphyrinates with Nitrite

Habib Nasri,[†,‡] Mary K. Ellison,[†] Carsten Krebs,[§] Boi Hanh Huynh,[§] and W. Robert Scheidt*[,†]

Contribution from the Department of Chemistry and Biochemistry, University of Notre Dame, Notre Dame, Indiana 46556, and Department of Physics, Emory University, Atlanta, Georgia 30322

Received January 13, 2000

Abstract: The reaction of the four-coordinate picket fence iron(II) porphyrin complex [Fe(TpivPP)] with cryptand-solubilized KNO_2 yields the five-coordinate porphyrin species $[Fe(TpivPP)(NO_2)]^-$. The six-coordinate complexes, $[Fe(TpivPP)(NO_2)(PMS)]^-$ and $[Fe(TpivPP)(NO_2)(Py)]^-$, are obtained when pentamethylene sulfide or pyridine is added anaerobically to the preformed five-coordinate porphyrin species. These novel species are characterized by UV−vis, IR, and Mössbauer spectroscopies as well as single-crystal structure determinations. The Mössbauer investigation shows that the isomer shifts and quadrupole splittings for $[Fe(TpivPP)(NO_2)(PMS)]^-$ and $[Fe(TpivPP)(NO_2)(Py)]^-$ are typical for six-coordinate, low-spin ($S = 0$) iron(II) porphyrinate complexes. This is in distinct contrast to the unusually large quadrupole splitting of the five-coordinate species $[Fe(TpivPP)(NO_2)]^-$. The molecular structures of $[Fe(TpivPP)(NO_2)(PMS)]^-$ and $[Fe(TpivPP)(NO_2)(Py)]^-$ show that the nitro groups are inside the "pocket" of the porphyrin trans to the neutral sulfur- or nitrogen-donating axial ligand. In all species, the projection of the nitrite ion onto the porphyrin plane bisects a N_p-Fe-N_p angle. In the pyridine derivative, the dihedral angle between the two axial ligand planes is 81.4°. In the pentamethylene sulfide derivative, $Fe-N_p = 1.990(6)$ Å, $Fe-N(NO_2) = 1.937(3)$ Å, and $Fe-S(PMS) = 2.380(2)$ Å, while in the pyridine derivative $Fe-N_p = 1.990(15)$ Å, $Fe-N(NO_2) = 1.951(5)$ Å, and $Fe-N(Py) = 2.032(5)$ Å. In $[Fe(TpivPP)(NO_2)]^-$, $Fe-N_p$ is 1.970(4) Å while $Fe-N(NO_2)$ is a very short 1.849(6) Å. The structural and spectroscopic data are interpreted as showing a significant difference in the $[Fe-NO_2]$ π interaction on change in coordination number.

Introduction

Nitrite ion reacts with both iron(II) and iron(III) hemoproteins including heme cd_1 nitrite reductase in many species of denitrifying bacteria. The enzyme catalyzes the single-electron reduction of nitrite to nitric oxide. Nitrite binds to the reduced enzyme to make a six-coordinate complex with histidine as the sixth ligand.[1] Assimilatory nitrite reductases serve to convert nitrite to ammonia using a siroheme (an isobacteriochlorin-type heme) and an Fe_4S_4 cluster prosthetic group. The mechanism by which this enzyme catalyzes the six-electron reduction without release of intermediates is still unclear.[2] Nitrite ion is also involved in the commercial application of meat curing,[3] which involves the binding of nitrite to heme proteins.

We have been concerned with the interesting bonding capabilities of nitrite ion. Our previous EPR and Mössbauer spectroscopic studies of ferric and ferrous porphyrinato nitrite complexes help define the electronic structure at iron and the bonding interactions of nitrite. EPR parameters show that, in the bis-nitrite species $[Fe(TpivPP)(NO_2)_2]^-$,[4] the presence of two trans axial nitrite ligands leads to a very large rhombicity parameter, as described by Blumberg and Peisach.[5] One of the nitrite ions in $[Fe^{III}(TpivPP)(NO_2)_2]^-$ can be replaced by neutral donor ligands to give the mixed-ligand species $[Fe^{III}(TpivPP)(NO_2)(HIm)]$ and $[Fe^{III}(TpivPP)(NO_2)(Py)]$.[6] In these mixed-ligand species it was found that the π-accepting nitrite ligand dominated the bonding and that the rhombicity, although still quite large, is greatly diminished from the bis-nitrite species. A species can be made with a thiolate ligand trans to nitrite.[7] The nitro ligand again dominates the bonding, but the thiolate likely makes a contribution to the large rhombicity revealed by EPR. Mössbauer measurements are consistent with these large rhombicities. All of these six-coordinate nitrite species have quadrupole splitting parameters greater than 2.0 mm/s, indicating a substantial difference in energy between the d_{xz} and d_{yz} orbitals. Nitrite is certainly acting as a strong π-accepting ligand.

Both iron(II) and iron(III) nitrosyl species with nitrite trans to the nitrosyl ligand can be synthesized. We have reported the structures and physical properties of two forms of the iron(II)

* To whom correspondence should be addressed.
† University of Notre Dame.
‡ Present address: Faculté des Sciences de Monastir, 5000 Monastir, Tunisia.
§ Emory University.

(1) Fülöp, V.; Moir, J. W. B.; Ferguson, S. J.; Hajdu, J. *Cell* **1995**, *81*, 369.

(2) (a) Vega, J. M.; Kamin, H. *J. Biol. Chem.* **1977**, *252*, 896. (b) Aparicio, P. J.; Knaff, D. B.; Malkin, R. *Arch. Biochem. Biophys.* **1975**, *169*, 102. (c) Coleman, K. J.; Cornish-Bowden, A.; Cole, J. A. *Biochem. J.* **1978**, *175*, 483.

(3) (a) Tsukahara, K.; Yamamoto, Y. *J. Biochem. (Tokyo)* **1983**, *93*, 15. (b) Fox, J. B.; Thomson, J. S. *Biochemistry* **1963**, *2*, 465. (c) Giddings, G. G. *J. Food Sci.* **1977**, *42*, 288. (d) Cassens, R. G.; Greaser, M. L.; Ito, T.; Lee, M. *Food Technol.* **1979**, *33*, 46.

(4) Nasri, H.; Goodwin, J. A.; Scheidt, W. R. *Inorg. Chem.* **1990**, *29*, 185.

(5) Blumberg, W. E.; Peisach, J. *Adv. Chem. Ser.* **1971**, *100*, 271.

(6) Nasri, H.; Wang, Y.; Huynh, B. H.; Walker, F. A.; Scheidt, W. R. *Inorg. Chem.* **1991**, *30*, 1483.

(7) Nasri, H.; Haller, K. J.; Wang, Y.; Huynh, B. H.; Scheidt, W. R. *Inorg. Chem.* **1992**, *31*, 3459.

10.1021/ja000149a CCC: $19.00
Published on Web 10/21/2000

complex $[Fe(TpivPP)(NO_2)(NO)]^-$.[8] The two crystalline forms differ in the relative axial ligand orientations. The planes defined by the axial ligand NO_2^- and the nitrosyl Fe−N−O plane have either perpendicular or parallel relative orientations. The two different ligand orientations have an effect on the electronic structure at iron, as shown by Mössbauer spectroscopy. The form with perpendicular ligand planes maximizes the π-bonding since each of the two ligands interacts with a distinct iron d_π orbital, while in the parallel form the two coplanar ligands are competing for π-bonding. Several iron(III) species, $[Fe(Porph)(NO_2)(NO)]$,[9] have also been synthesized. Mössbauer measurements show that the quadrupole splitting parameter is significantly diminished from all other porphyrinato nitrite species. The linear nitrosyl group trans to the nitrite leads to a more nearly equivalent energy of the two d_π orbitals. The presence of the nitrosyl group also significantly decreases the isomer shift with respect to six-coordinate iron(III) nitrite species, further confirming its dominance in the bonding.

A five-coordinate iron(III) nitrite species has not yet been isolated, apparently because of its high reactivity.[10] Such a species has been detected in solution with EPR spectroscopy and found to be low spin.[11] However, we have previously communicated that the five-coordinate iron(II) nitrite species $[Fe(TpivPP)(NO_2)]^-$ can be isolated and that it has a low-spin state.[12] The low-spin state is achieved with the presence of only a single axial ligand. The molecular structure determination showed that the axial $Fe-N(NO_2)$ bond length is quite short, at 1.849(6) Å. Mössbauer measurements for the complex showed a very large quadrupole splitting constant of 2.28 mm/s. The interpretation of this very large quadrupole splitting for low-spin iron(II) is that the axial N-bonded nitrite ligand is an extremely strong π acceptor with iron. However, only one of the two iron d_π orbitals can interact, and hence a large difference in the energies of the originally degenerate d_{xz} and d_{yz} orbitals results. This d_π energy difference (rhombicity) is manifested in the Mössbauer spectrum as the unusually large quadrupole splitting value.

We report herein the results of the reaction of $[Fe(TpivPP)(NO_2)]^-$ with the neutral sulfur- and nitrogen-donating axial ligands pentamethylene sulfide and pyridine. The products are the six-coordinate mixed-axial ligand complexes $[Fe(TpivPP)(NO_2)(PMS)]^-$ and $[Fe(TpivPP)(NO_2)(Py)]^-$. These five- and six-coordinate iron(II) species are characterized by their distinctive UV−vis spectra. Single-crystal structure determinations and Mössbauer measurements have been done on all three iron(II) nitrite species. The differences in the bonding between iron(II) and nitrite in the complete set of iron(II) derivatives show large variations that range from strong π-acceptor behavior in the five-coordinate complex to weaker π-acceptor character in the present six-coordinate species to even smaller apparent π interaction in the mixed nitrite/nitrosyl complexes. We suggest that the term highly "variable π-bonding" be applied to the interaction between nitrite and iron(II) to recognize this divergent behavior.

Experimental Section

General Information. Chlorobenzene was purified by washing with sulfuric acid and then distilled over P_2O_5. Pentane and hexanes were distilled over CaH_2. All solvents were degassed before use by three freeze/pump/thaw cycles. Pyridine was distilled under vacuum and used immediately. KNO_2 was recrystallized twice from distilled water, dried overnight at about 75 °C, and stored under argon. Kryptofix−222 (Aldrich) was recrystallized from benzene (dried by distillation over sodium/benzophenone) and stored under argon in the dark. All other chemicals were used as received from Aldrich or Fisher. All manipulations were carried out under argon using a double-manifold vacuum line, Schlenkware, and cannula techniques. IR spectra were recorded on a Perkin-Elmer 883 IR spectrophotometer as KBr pellets; electronic spectra were recorded on a Perkin-Elmer Lambda 19 UV/vis/near-IR spectrometer. Samples for Mössbauer spectroscopy were prepared either by strongly tamping a crystalline solid into Teflon sample holders or by immobilizing the crystalline material (crystals not ground) in paraffin wax (mp 78 °C) in an inert atmosphere drybox. Mössbauer spectra were recorded in a weak-field spectrometer equipped with a Janis 8DT variable-temperature cryostat operating in a constant acceleration mode in a transmission geometry.[13] The zero velocity of the spectra refers to the centroid of a room-temperature spectrum of a metallic iron foil. The free base, $(H_2TpivPP)$,[14] and the corresponding iron(III) chloro and triflato derivatives, were synthesized according to literature methods.[15,16]

Preparation of $[K(222)][Fe(TpivPP)(NO_2)]\cdot H_2O\cdot C_6H_5Cl$. $[Fe(TpivPP)(SO_3CF_3)(H_2O)]$ (100 mg, 0.08 mmol) and ~1 mL of zinc amalgam were stirred for 1 h under argon in 10 mL of C_6H_5Cl. This deep red solution of [Fe(II)TpivPP] was then filtered into a second solution that was made by stirring overnight 300 mg (0.8 mmol) of Kryptofix−222 and 207 mg of KNO_2 (2.4 mmol) in 10 mL of C_6H_5Cl. The solution was filtered, and crystals of the complex were prepared by slow diffusion of pentane into the chlorobenzene solution. UV−vis in C_6H_5Cl: λ_{max} (log ϵ) 433 (sh) (4.94); 444 (5.12); 543 (3.89); 567 (4.02); 608 (3.59); 653 (3.10).

Preparation of $[K(H_2O)(222)][Fe(TpivPP)(NO_2)(PMS)]\cdot C_6H_5Cl$. Pentamethylene sulfide (1 mL, 9.6 mmol) was added to the red-yellow solution which contains the iron(II) five-coordinate species $[Fe(TpivPP)(NO_2)]^-$ as described above. The color changed to bright-red, and the result of this reaction is the six-coordinate product, $[Fe(TpivPP)(NO_2)(PMS)]^-$. Single crystals of this complex were prepared by slow diffusion of dry pentane into the chlorobenzene solution. UV−vis in C_6H_5Cl: λ_{max} (log ϵ) 418 (sh) (4.88); 432 (5.07); 537 (4.18); 558 (sh) (3.81); 653 (3.12). IR (KBr): $\nu(NO_2^-)$ 1349 (m), 1295 (m) cm^{-1}.

Preparation of $[K(222)]_2(NO_2^-,NO_3^-)[Fe(TpivPP)(NO_2)(Py)]\cdot 2H_2O$. Pyridine (1.0 mL, 12.4 mmol) was added to the red-yellow solution which contains the iron(II) five-coordinate species $[Fe(TpivPP)(NO_2)]^-$ as described above. The color changed immediately to a lighter red as a result of the formation of the six-coordinate product $[Fe(TpivPP)(NO_2)(Py)]^-$. Single crystals of this complex were prepared by slow diffusion of dry pentane into chlorobenzene solution. X-ray analysis showed that, in addition to the desired complex, an additional molecule of 222 as the potassium NO_2^-/NO_3^- salt was found to be cocrystallized in the cell. UV−vis in C_6H_5Cl: λ_{max} (log ϵ) 413 (sh) (4.83); 430 (5.23); 533 (4.21); 560 (sh) (3.66); 653 (2.83). IR (KBr): $\nu(NO_2^-)$ 1289 (w), 1354 (m) cm^{-1}.

X-ray Structure Determinations. The data for the complex $[Fe(TpivPP)(NO_2)]^-$ were collected on an Enraf-Nonius CAD4 diffractometer with Mo Kα radiation. Data were collected at 123 K. Intensity data were measured with $\theta-2\theta$ scans. The intensity data were

(8) Nasri, H.; Ellison, M. K.; Chen, S.; Huynh, B. H.; Scheidt, W. R. *J. Am. Chem. Soc.* **1997**, *119*, 6274.

(9) Ellison, M. K.; Schulz, C. E.; Scheidt, W. R. *Inorg. Chem.* **1999**, *38*, 100.

(10) Finnegan, M. G.; Lappin, A. G.; Scheidt, W. R. *Inorg. Chem.* **1990**, *29*, 181.

(11) Munro, O. Q.; Scheidt, W. R. *Inorg. Chem.* **1998**, *37*, 2308.

(12) Nasri, H.; Wang, Y.; Huynh, B. H.; Scheidt, W. R. *J. Am. Chem. Soc.* **1991**, *113*, 717.

(13) Kretchmar, S. A.; Teixeira, M.; Huynh, B. H.; Raymond, K. N. *Biol. Met.* **1988**, *1*, 26.

(14) Abbreviations: Porph, a generalized porphyrin dianion; TpivPP, dianion of (α,α,α,α -tetrakis(*o*-pivalamidophenyl)porphyrin; T*p*-OCH_3PP, dianion of *meso*-tetra-*p*-methoxyphenylporphyrin; PMS, pentamethylene sulfide; Py, pyridine; THT, tetrahydrothiophene; THF, tetrahydrofuran; HIm, imidazole; 1-MeIm, 1-methylimidazole; 2-MeIm, 2-methylimidazole; 1,2-Me_2Im, 1,2-dimethylimidazole; 4-MePip, 4-methylpiperidine; Pz, pyrazole; Kryptofix−222 or 222, 4,7,13,16,21,24-hexaoxo-1,10-diazabicyclo[8.8.8]-hexacosane; N_p, porphyrinato nitrogen.

(15) Collman, J. P.; Gagne, R. R.; Halbert, T. R.; Lang, G.; Robinson, W. T. *J. Am. Chem. Soc.* **1975**, *97*, 1427.

(16) Gismelseed; A.; Bominaar, E. L.; Bill, E.; Trautwein, A. X.; Winkler, H.; Nasri, H.; Doppelt, P.; Mandon, D.; Fischer, J. Weiss, R. *Inorg. Chem.* **1990**, *29*, 2741.

Table 1. Crystallographic Details for the Iron Nitrite Derivatives

	$[Fe(TpivPP)(NO_2)]^-$	$[Fe(TpivPP)(NO_2)(PMS)]^-$	$[Fe(TpivPP)(NO_2)(Py)]^-$
formula	$[K(O_6N_2C_{18}H_{36}][Fe(O_4N_8C_{64}H_{64})(NO_2)]\cdot H_2O\cdot C_6H_5Cl$	$[K(O_6N_2C_{18}H_{36})(H_2O)_{0.25}][Fe(O_4N_8C_{64}H_{64})(NO_2)(SC_5H_{10})]\cdot C_6H_5Cl$	$\{[K(O_6N_2C_{18}H_{36})]_2[(NO_3^-)_{0.6}(NO_2^-)_{0.4}]\}\cdot[Fe(O_4N_8C_{64}H_{64})(NO_2)(NC_5H_5)]\cdot 2H_2O$
fw	1657.29	1733.96	2038.9
a, Å	17.715(7)	19.101(6)	19.48(3)
b, Å	21.341(5)	19.709(16)	23.62(3)
c, Å	22.838(11)	24.394(4)	24.43(3)
β, deg	101.86(3)	104.693(9)	102.99(14)
V, Å^3	8450	8883(12)	10953(27)
Z	4	4	4
space group	$P2_1/n$	$P2_1/n$	$P2_1/a$
temp, K	123	127	127
D_c, g/cm^3	1.30	1.29	1.24
μ, mm^{-1}	0.324	0.330	0.255
R_1	0.079	0.050	$R_1 = 0.079$, w$R_2 = 0.196$
R_2	0.087	0.058	$R_1 = 0.112$, w$R_2 = 0.227$

reduced with the Blessing[17] data reduction programs with corrections for Lorentz and polarization. The two six-coordinate structure determinations were carried out on an Enraf-Nonius FAST area-detector diffractometer with a Mo rotating anode source ($\bar{\lambda} = 0.71073$ Å). Our detailed methods and procedures for small-molecule X-ray data collection with the FAST system have been described previously.[18] Data collections were performed at 127(2) K. Brief crystal data are listed in Table 1. Complete crystallographic details for the structures are included in the Supporting Information (Tables S1, S7, and S13).

A dark purple crystal of $[K(222)][Fe(TpivPP)(NO_2)]\cdot H_2O\cdot C_6H_5Cl$ with dimensions $0.59 \times 0.53 \times 0.17$ mm^3 was used for the structure determination. The structure was solved in the space group $P2_1/n$ using the coordinates for the iron porphyrin and [K(222)] cation of the isomorphous nitrato[19] and acetato[20] structures. Subsequent difference Fourier syntheses led to location of the remaining atoms.[21] Final atomic coordinates, anisotropic thermal parameters for all heavy atoms, and fixed hydrogen atom coordinates are available as Supporting Information (Tables S2, S5, and S6).

A dark purple crystal of $[K(H_2O)(222)][Fe(TpivPP)(NO_2)(PMS)]\cdot C_6H_5Cl$ with dimensions $0.63 \times 0.41 \times 0.48$ mm^3 was used for the structure determination. The structure was solved in the centrosymmetric space group $P2_1/n$ using SHELXS-86. Subsequent difference Fourier syntheses led to location of almost all heavy atoms. After full-matrix least-squares refinement was carried to convergence, a difference Fourier suggested possible locations for about 80% of the hydrogen atoms of the Kryptofix−222 and the porphyrin. These hydrogen atoms were included in subsequent cycles of the least-squares refinement as fixed, idealized contributions (C−H = 0.95 Å, N−H = 0.90 Å, B(H) = B(C,N) × 1.3). Final cycles of full-matrix least-squares refinement used anisotropic temperature factors for all heavy atoms. At convergence, $R_1 = 0.050$ and $R_2 = 0.058$, and the final data/variables ratio was 11.1. A final difference Fourier map was judged to be significantly free of features, with the largest positive peak having a height of 0.55 e/Å^3. Final atomic coordinates, anisotropic thermal parameters for all heavy atoms, and fixed hydrogen atom coordinates are available as Supporting Information (Tables S8, S11, and S12).

A dark purple crystal of $[K(222)]_2(NO_2^-,NO_3^-)[Fe(TpivPP)(NO_2)(Py)]\cdot 2H_2O$ with dimensions of $0.65 \times 0.31 \times 0.28$ mm^3 was used for the structure determination. The structure was solved in the centrosymmetric space group $P2_1/a$ with the direct methods program MULTAN. Subsequent difference Fourier syntheses (using SHELXL-93[22]) led to location of all heavy atoms of the $[Fe(TpivPP)(NO_2)(Py)]^-$ ion and the counterion, which presents two serious disorder problems. The counterion was expected to be a single molecule of potassium−Kryptofix−222; however, the difference Fourier map showed the presence of two distinct potassium−222 cations. The two cations were found to be linked together by an adventitious nitrite/nitrate anion. The balance of charge is as expected. One potassium−222 cation is completely ordered. The second potassium−222 cation is disordered over two positions as well as having minor disorder of several methylene oxide groups within each orientation. This molecule is connected to the ordered molecule by a disordered bridging nitrite/nitrate anion. A complete description of the disorder including figures can be found in the Supporting Information. After full-matrix least-squares refinement was carried to convergence, a difference Fourier suggested possible locations for almost all hydrogen atoms of the first Kryptofix−222 and about 60% of the hydrogen atoms of the porphyrin. These hydrogen atoms were included in subsequent cycles of the least-squares refinement as fixed, idealized contributions. Final cycles of full-matrix least-squares refinement used anisotropic temperature factors for all heavy atoms except the second position of the disordered potassium atom K2Y and all atoms of the two confirmations *X* and *Y* of the disordered Kryptofix−222. The refinement converged to final values $R_1 = 0.079$ and wR_2 0.196 ($I > 2\sigma(I)$). The maximum electron density on the final difference Fourier map was 1.26 e/Å^3 at a distance of 1.14 Å from the O5X atom and −0.63 e/Å^3, respectively. Final atomic coordinates, anisotropic thermal parameters for all heavy atoms, and fixed hydrogen atom coordinates are available as Supporting Information (Tables S14, S17, and S18).

Results

The syntheses of $[Fe(TpivPP)(NO_2)]^-$ and the six-coordinate iron(II) nitrite species, $[Fe(TpivPP)(NO_2)(PMS)]^-$ and $[Fe(TpivPP)(NO_2)(Py)]^-$, are straightforward yet require substantial care due to the oxygen sensitivity of these species in solution. The species $[Fe(TpivPP)(NO_2)]^-$ was prepared by addition of [Fe(II)TpivPP] (made by reduction of the iron(III) species, $[Fe(TpivPP)(SO_3CF_3)(H_2O)]$, with zinc amalgam) to excess KNO_2

(17) Blessing, R. H. *Crystallogr. Rev.* **1987**, *1*, 3.
(18) Scheidt, W. R.; Turowska-Tyrk, I. *Inorg. Chem.* **1994**, *33*, 1314.
(19) Nasri, H.; Reed, C. A.; Scheidt, W. R., unpublished results.
(20) Nasri, H.; Fischer, J.; Weiss, R. *J. Am. Chem. Soc.* **1987**, *109*, 2549.
(21) Programs used in this study include the following: (a) Zalkin's FORDAP for difference Fourier syntheses. (b) Local modified least-squares refinement: Lapp, R. L.; Jacobson, R. A. *ALLS*, a generalized crystallographic least-squares program; IS-4708 UC-4; National Technical Information Services: Springfield, VA. (c) Busing and Levy's ORFFE and ORFLS, and Johnson's ORTEPII. (d) Atomic form factors were from the following: Cromer, D. T.; Mann, J. B., *Acta Crystallogr., Sect. A* **1968**, *24*, 321. Real and imaginary corrections for anomalous dispersion in the form factor of iron, the potassium and the chlorine atoms were from the following: Cromer, D. T.; Liberman, D. J. *J. Chem. Phys.* **1970**, *53*, 1891. Scattering factors for hydrogen were from the following: Stewart, R. F.; Davidson, E. R.; Simpson, W. T. *J. Chem. Phys.* **1970**, *42*, 3175. (e) Direct methods program SHELXS-86: Sheldrick, G. M. *Acta Crystallogr.* **1990**, *A46*, 467. (f) Direct method program MULTAN: Main, P.; Hull, S. E.; Lessinger, L.; Germain, G.; Declerq, J. P.; Woolfson, M. M. *Multan*, a system of computer programs for the automatic solution of the crystal structures from X-ray diffraction data; Universities of York, U.K., and Louvain, Belgium. (g) SHELXL-93: Sheldrick, G. M. *J. Appl. Crystallogr.*, in preparation.

(22) $R_1 = \sum||F_o| - |F_c||\sum|F_o|$ and w$R_2 = \{\sum[w(F_o^2 - F_c^2)^2]/\sum[wF_o^4]\}^{1/2}$. The conventional *R*-factors R_1 are based on *F*, with *F* set to zero for negative F^2. The criterion of $F^2 > 2\sigma(F^2)$ was used only for calculating R_1. *R*-factors based on F^2 (wR_2) are statistically about twice as large as those based on *F*, and *R*-factors based on *all* data will be even larger.

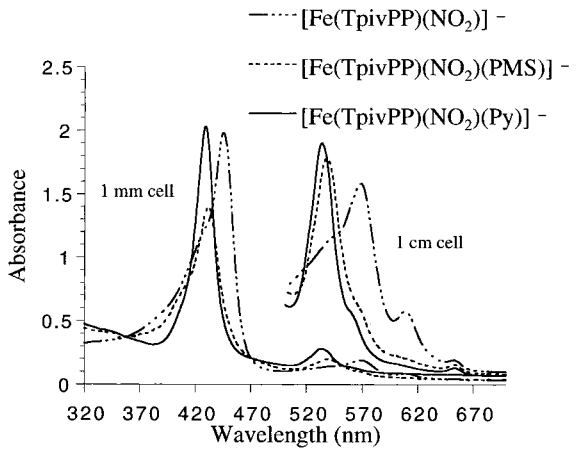

Figure 1. UV−vis spectra of the nitrite derivatives taken under argon in chlorobenzene solution. $[Fe(TpivPP)(NO_2)]^-$ (—•••—), concentration $= 0.148 \times 10^{-3}$ M; $[Fe(TpivPP)(NO_2)(PMS)]^-$ (•••), $C = 0.119 \times 10^{-3}$ M; $[Fe(TpivPP)(NO_2)(Py)]^-$ (—), $C = 0.116 \times 10^{-3}$ M.

solubilized with Kryptofix−222. The syntheses of the six-coordinate species involves the simple addition of excess neutral ligand to the five-coordinate species $[Fe(TpivPP)(NO_2)]^-$ prepared in situ. Kryptofix−222 and KNO_2 must be carefully recrystallized to remove halide impurities known to coordinate strongly to iron(II) species.

The five- and six-coordinate iron(II) nitrite species are characterized by UV−vis spectroscopy. The spectra (Figure 1) were obtained in chlorobenzene solution in a specially designed combined 1- and 10-mm inert atmosphere cell. The five-coordinate and six-coordinate nitrite species were also isolated as crystalline solids and studied by X-ray diffraction. These anions were crystallized as potassium−222 salts with varying amounts of water and other solvents present in the unit cell. ORTEP diagrams of $[Fe(TpivPP)(NO_2)]^-$, $[Fe(TpivPP)(NO_2)(PMS)]^-$, and $[Fe(TpivPP)(NO_2)(Py)]^-$ are given in Figures 2−4. In all three structures, the nitrite ion is located in the binding pocket formed by the pivalamide groups. The nitrite ion nearly bisects the N_p-Fe-N_p angle in the three derivatives. The angles and orientation of the nitrite ion with respect to the porphyrin plane are given in Figure 5. The displacements of each atom, in units of 0.01 Å, from the 24-atom porphyrin core are given. In all three species the view is from the picket side (nitrite side) of the plane, and positive values of displacement are above the page. Also displayed in this figure are the average bond parameters for each type of bond and angle. A summary of individual bond lengths and angles is given in Table 2. Full listings of the bond parameters for all three structures are given in the Supporting Information (Tables S3,S4; S9,S10; S15,S16). The labeling scheme used is displayed in the ORTEP diagrams (Figures 2−4).

The equatorial $Fe-N_p$ bond distance average is 1.970(4) Å for $[Fe(TpivPP)(NO_2)]^-$ and 1.990 Å for both six-coordinate derivatives. The $Fe-N(NO_2)$ bond length is 1.849(6) Å in $[Fe(TpivPP)(NO_2)]^-$ and increases upon coordination of the sixth ligand to 1.937(3) and 1.951(5) Å for $[Fe(TpivPP)(NO_2)(PMS)]^-$ and $[Fe(TpivPP)(NO_2)(Py)]^-$, respectively. The Fe−S(PMS) bond length is 2.380(2) Å, and Fe−N(Py) is 2.032(5) Å.

In the five-coordinate derivative, the iron atom is out of the 24-atom mean plane toward the nitrite ligand by 0.18 Å. In the six-coordinate derivatives, the neutral ligand is trans to the nitrite, and the iron atom is displaced very slightly in the direction of the neutral ligand. In the pyridine species, the dihedral angle between the plane formed by the nitrite ion and the pyridine ligand plane is 81.4°.

All three structures contain a potassium−222 counterion to balance the charge of the (nitro)(porphyrinato)iron(II) anion. ORTEP diagrams of each counterion are supplied in the Supporting Information (Figures S1−S4). The potassium ion of the Kryptofix−222 molecule in $[Fe(TpivPP)(NO_2)]^-$ is eight coordinate. The average K−O(222) distance is 2.83(3) Å, and the K−N(222) average is 3.04(2) Å. In addition, there is a fully occupied adventitious water molecule in the ligand binding pocket with $O(w)-O(NO_2)$ distances of 3.17 and 3.36 Å. The potassium ion of the Kryptofix−222 complex in the pentamethylene sulfide derivative is nine coordinate. Six oxygen atoms and two nitrogen atoms from the 222 molecule plus an oxygen of a water molecule make up the coordination sphere. The water molecule, however, is present only 25% of the time. The average K−O(222) distance is 2.84(2) Å, and the K−N(222) average is 2.986(6) Å. The K−O(w) distance is 2.646(15) Å. In the pyridine derivative there is an additional molecule of potassium−222 which is charge-balanced by a mixture of adventitious nitrite and nitrate ions. This molecule is substantially disordered, and a description of the disorder is supplied in the Supporting Information. In the ordered potassium−222 molecule, the average K−O(222) distance is 2.85(9) Å, and the K−N(222) average is 3.07(2) Å.

Solid-state Mössbauer measurements were done on all three compounds. The data are summarized in Table 3, along with Mössbauer parameters for related iron(II) and iron(III) porphyrin species. The quadrupole splitting constant for $[Fe(TpivPP)(NO_2)]^-$ is 2.28 mm/s at 4.2 K. The isomer shifts are nearly identical for all three species (∼0.41 mm/s.). The quadrupole splittings for $[Fe(TpivPP)(NO_2)(PMS)]^-$ and $[Fe(TpivPP)(NO_2)(Py)]^-$ are 1.18 and 0.93 mm/s, respectively. Figure 6 shows Mössbauer spectra of $[Fe(TpivPP)(NO_2)]^-$ (A), at 4.2 K in zero applied magnetic field. The Mössbauer spectra of the six-coordinate complexes $[Fe(TpivPP)(NO_2)(Py)]^-$ (B) and $[Fe(TpivPP)(NO_2)(PMS)]^-$ (C) at 4.2 K are also shown in Figure 6. An extra quadrupole doublet, present in the spectrum of $[Fe(TpivPP)(NO_2)(PMS)]^-$, is that of $[Fe(TpivPP)(NO_2)]^-$ which corresponds to approximately 15% of the sample.

Discussion

The synthesis of $[Fe(TpivPP)(NO_2)]^-$ is straightforward and involves the addition of excess nitrite, solubilized by a crown ether, to the highly air-sensitive, four-coordinate iron(II) species [Fe(TpivPP)]. Although an excess of solubilized nitrite is present, the dianionic bis-nitro iron(II) species has never been observed. In contrast, the addition of excess solubilized nitrite to the iron(III) species $[Fe(TpivPP)(SO_3CF_3)(H_2O)]$ yields *only* the six-coordinate bis-nitro iron(III) species.[4] The analogous five-coordinate (nitro)iron(III) porphyrin species has not yet been isolated, even with limited nitrite concentrations. In addition to unfavorable binding equilibria that lead to six-coordinate bis-nitrite species, there is oxygen-atom-transfer chemistry that dominates the reactivity of the iron(III) porphyrin species in solution.[10,11,32] It was found that the iron(III) species undergo oxygen atom transfer from the iron-bound nitrite to free nitrite in solution, yielding the thermodynamically stable iron nitrosyl species.[10] Under these conditions, iron nitr*ate* species can also be isolated.[11] The high reactivity of the iron(III) species is in distinct contrast to the relative stability of the iron(II) species in the absence of oxygen. We see no evidence for oxygen-atom-transfer chemistry in solutions of $[Fe(TpivPP)(NO_2)]^-$. Presumably, the iron(III) six-coordinate bis-nitro species, $[Fe(TpivPP)(NO_2)_2]^-$,[4] can be readily isolated because the nitrite ligands are protected from oxygen atom transfer by the pocket formed

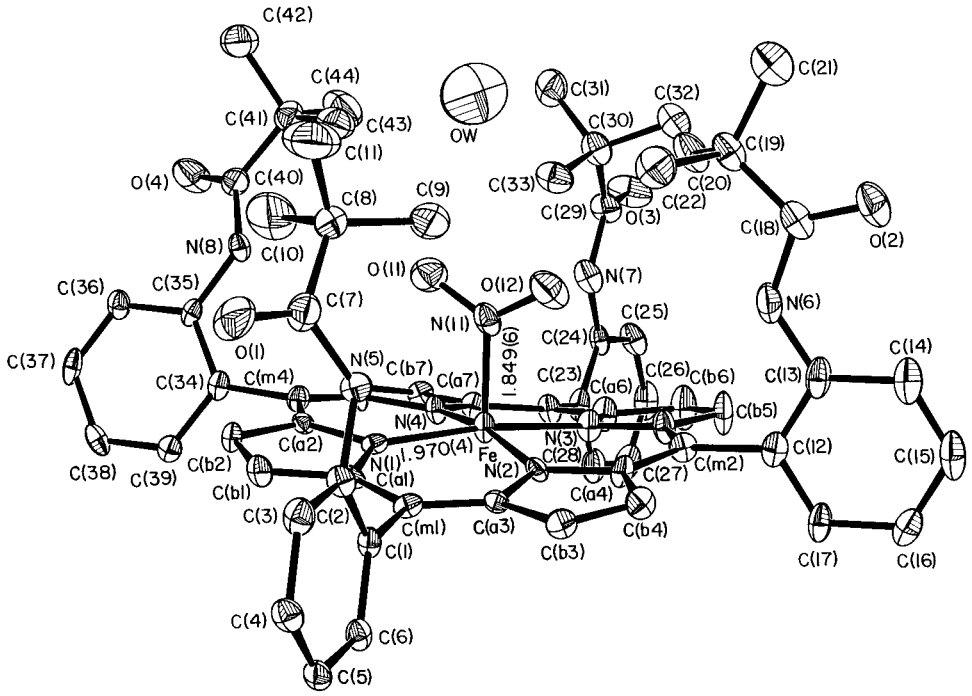

Figure 2. ORTEP diagram illustrating the molecular structure of $[Fe(TpivPP)(NO_2)]^-$ (30% probability ellipsoids). The labels of the crystallographically unique atoms are shown.

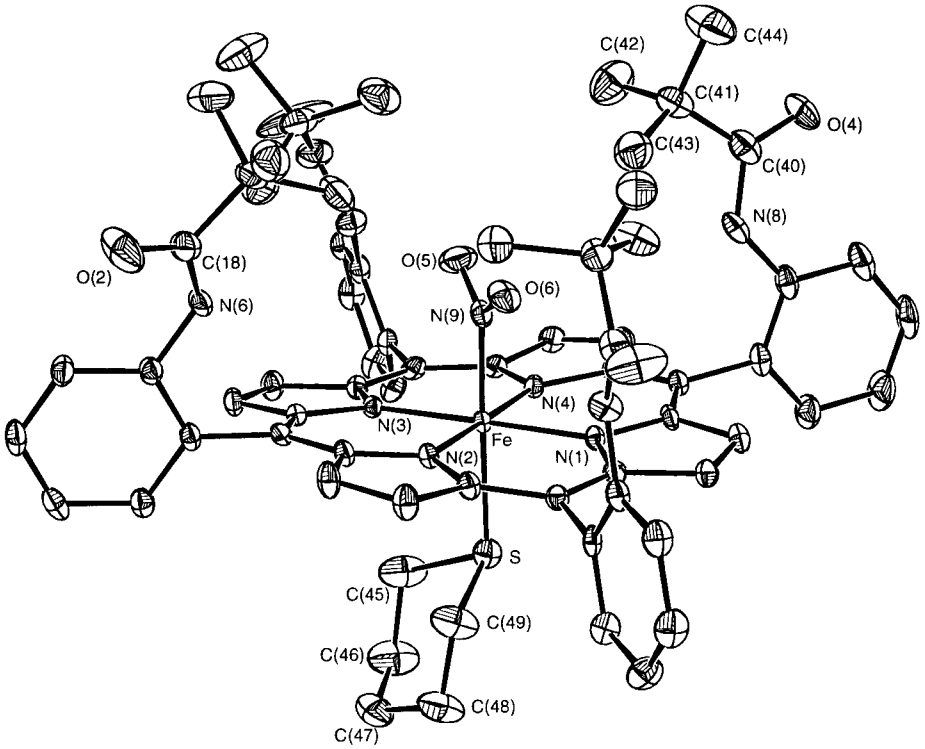

Figure 3. ORTEP diagram illustrating the molecular structure of $[Fe(TpivPP)(NO_2)(PMS)]^-$ (30% probability ellipsoids). The labels of the crystallographically unique atoms are shown.

by the pivalamide groups on one side and a potassium−(18-crown-6) which closely approaches the nitrite ion on the open-face side of the molecule. Both of these features restrict access to the nitrite ligands and so prevent interaction of free nitrite in solution and the bound ligands. However, even with the use of the protected porphyrin strategy, a five-coordinate (nitro)iron(III) species cannot be isolated.[11]

We first consider the characterization data for $[Fe(TpivPP)(NO_2)]^-$. The electronic spectrum of $[Fe(TpivPP)(NO_2)]^-$ is shown in Figure 1. The strongly red-shifted Soret (444 nm) and visible bands (567 and 608 nm) are quite different from those of any other (nitro)iron porphyrin species thus far characterized.

(23) The number in parentheses following each averaged value is the estimated standard deviation calculated on the assumption that all values are drawn from the same population.

(24) Safo, M. K.; Nesset, M. J. M.; Walker, F. A.; Debrunner, P. G.; Scheidt, W. R. *J. Am. Chem. Soc.* **1997**, *119*, 9438.

(25) Kobayashi, H.; Maeda, Y.; Yanagawa, Y. *Bull. Chem. Soc. Jpn.* **1970**, *43*, 2342.

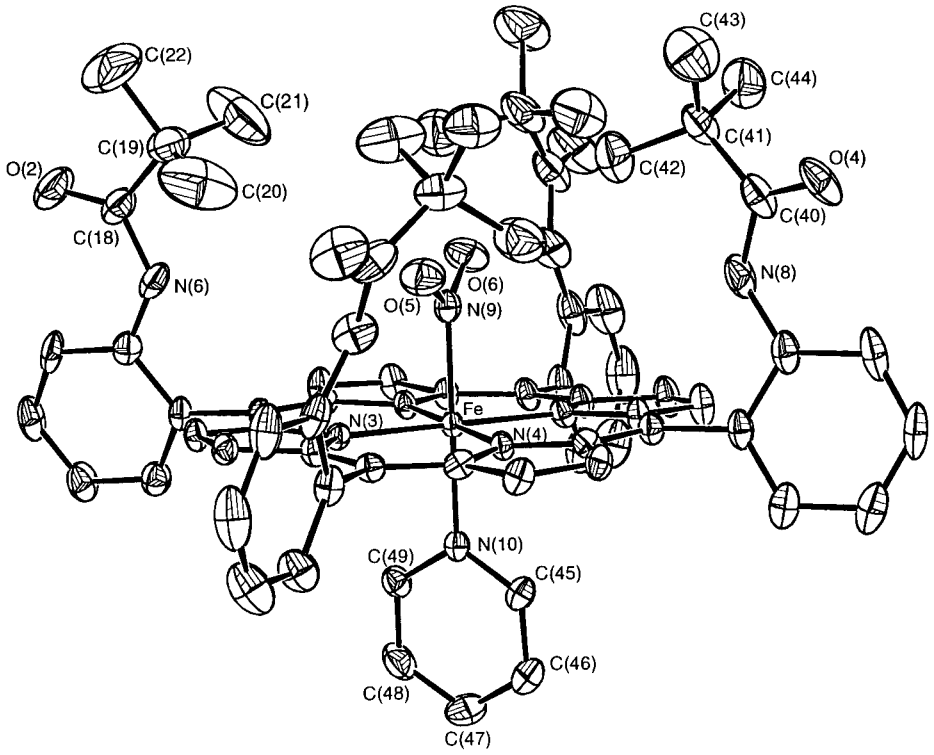

Figure 4. ORTEP diagram illustrating the molecular structure of $[Fe(TpivPP)(NO_2)(Py)]^-$ (50% probability ellipsoids). The labels of the crystallographically unique atoms are shown. The nearly perpendicular orientation of the nitrite ion plane and the pyridine plane is evident.

Similar red-shifted Soret and visible bands are also seen for high-spin five-coordinate anionic iron(II) species.[34−36] The spectrum of $[Fe(TpivPP)(NO_2)]^-$ is quite different from those of five-coordinate $\{FeNO\}^7$ species that typically have a Soret band at 407 nm and a broad visible band at 538 nm.

Figure 2 is an ORTEP drawing showing the structure of five-coordinate $[Fe(TpivPP)(NO_2)]^-$. The axial $Fe-N(NO_2)$ bond length is very short at 1.849(6) Å, which is more than 0.1 Å shorter than that of any of the (nitro)iron(III) porphyrin species given in Table 2, where the range of $Fe-N(NO_2)$ bond lengths is 1.949(10)−1.998(2) Å. Unfortunately, a direct comparison to a five-coordinate iron(III) species cannot be made. The short axial bond length suggests that nitrite, when it is the sole axial ligand in this iron(II) species, is acting as a very strong π acceptor. The average $Fe-N_p$ bond length of 1.970(4) Å is also quite short, consistent with the small out-of-plane iron displacement of 0.18 Å. The porphyrin core is slightly ruffled, as can be seen in Figure 5 (top), which also leads to a shortening of the iron−porphyrin bond lengths. All of these geometric parameters are consistent with a low-spin-state assignment for the iron(II) atom in $[Fe(TpivPP)(NO_2)]^-$. The low-spin state of $[Fe(TpivPP)(NO_2)]^-$ further emphasizes the π-accepting ability of a single nitrite, which has a sufficient axial ligand field strength to give a low-spin complex. All previously structurally characterized five-coordinate iron(II) porphyrinate complexes with anionic ligands are high spin.[37]

Figure 5 (top) also shows the orientation of the N-coordinated nitrite ion with respect to the porphyrin ligand in $[Fe(TpivPP)(NO_2)]^-$. The dihedral angle between the nitrite ligand and the nearest $Fe-N_p$ vector is 40.4°. In fact, in all (nitro)iron porphyrinates, the nitrite ligand bisects the N_p-Fe-N_p bond angles to within a few degrees. This orientation is not the result of steric interactions but apparently strongly reflects a feature in the bonding interaction of nitrite with iron. The nitrite ligand and not the heme ligand determines the orientation of the two d_π orbitals to achieve the best π overlap. In other words, the lobes of the two d_π orbitals are parallel and perpendicular to the nitrite plane. This interpretation is supported by earlier Mössbauer spectra obtained on (nitro)iron(III) complexes in an applied magnetic field which requires a counterrotation of the $\tilde{\mathbf{g}}$ and $\tilde{\mathbf{A}}$ tensor axes for a good fit of the spectra.[6]

Mössbauer spectra for $[Fe(TpivPP)(NO_2)]^-$ were obtained at 4.2 K both in the absence and in the presence of a strong (8 T) magnetic field applied parallel to the γ-beam. The quadrupole splitting parameter (ΔE_Q) for $[Fe(TpivPP)(NO_2)]^-$ was found

(26) Dolphin, D.; Sams, J. R.; Tsin, T. B.; Wong, K. L. *J. Am. Chem. Soc.* **1976**, *98*, 6970.
(27) Collman, J. P.; Gagne, R. R.; Reed, C. A.; Halbert, T. R.; Lang, G.; Robinson, W. T. *J. Am. Chem. Soc.* **1975**, *97*, 1427.
(28) Safo, M. K.; Scheidt, W. R.; Gupta, G. P. *Inorg. Chem.* **1990**, *29*, 626.
(29) Settin, M. F.; Fanning, J. C. *Inorg. Chem.* **1988**, *27*, 1431.
(30) Boso, B.; Lang, G.; Reed, C. A. *J. Chem. Phys.* **1983**, *78*, 2561.
(31) Kent, T. A.; Spartalian, K.; Lang, G.; Yonetani, T. Reed, C. A.; Collman, J. P. *Biochim. Biophys. Acta* **1979**, *580*, 245.
(32) (a) O'Shea, S. K.; Wang, W.; Wade, R. S.; Castro, C. E. *J. Org. Chem.* **1996**, *61*, 6388. (b) Castro, C. E.; O'Shea, S. K. *J. Org. Chem.* **1995**, *60*, 1922.
(33) Collman, J. P.; Brauman, J. I.; Doxsee, K. M.; Halbert, T. R.; Bunnenberg, E.; Linder, R. E.; LaMar, G. N.; Gaudio, J. D.; Lang, G.; Spartalian, K. *J. Am. Chem. Soc.* **1980**, *102*, 4182.
(34) Mincey, T.; Traylor, T. G. *J. Am. Chem. Soc.* **1979**, *101*, 765.
(35) Mandon, D.; Ott-Woelfel, F.; Fischer, J.; Weiss, R.; Bill, E.; Trautwein, A. X. *Inorg. Chem.* **1990**, *29*, 2442.
(36) Schappacher, M.; Ricard, L.; Weiss, R.; Montiel-Montoya, R.; Gonser, U.; Bill, E.; Trautwein, A. X. *Inorg. Chim. Acta* **1983**, *78*, L9.
(37) Examples include the anions ethanethiolate,[38,39] chloride,[36] tetrafluorophenylthiolate,[36] phenoxide,[40] 2-methylimidazolate,[35] and acetate.[41]
(38) Caron, C.; Mitschler, A.; Rivère, G.; Ricard, L.; Schappacher, M.; Weiss, R. *J. Am. Chem. Soc.* **1979**, *101*, 7401.
(39) Schappacher, M.; Ricard, L.; Fischer, J.; Weiss, R.; Montiel-Montoya, R.; Bill, E.; Trautwein, A. X. *Inorg. Chem.* **1989**, *28*, 4639.
(40) Nasri, H.; Fischer, J.; Weiss, R.; Bill, E.; Trautwein, A. X. *J. Am. Chem. Soc.* **1987**, *109*, 2549.
(41) Bominaar, E. L.; Ding, X.; Gismelseed, A.; Bill, E.; Winkler, H.; Trautwein, A. X.; Nasri, H.; Fischer, J.; Weiss, R. *Inorg. Chem.* **1992**, *31*, 1845.

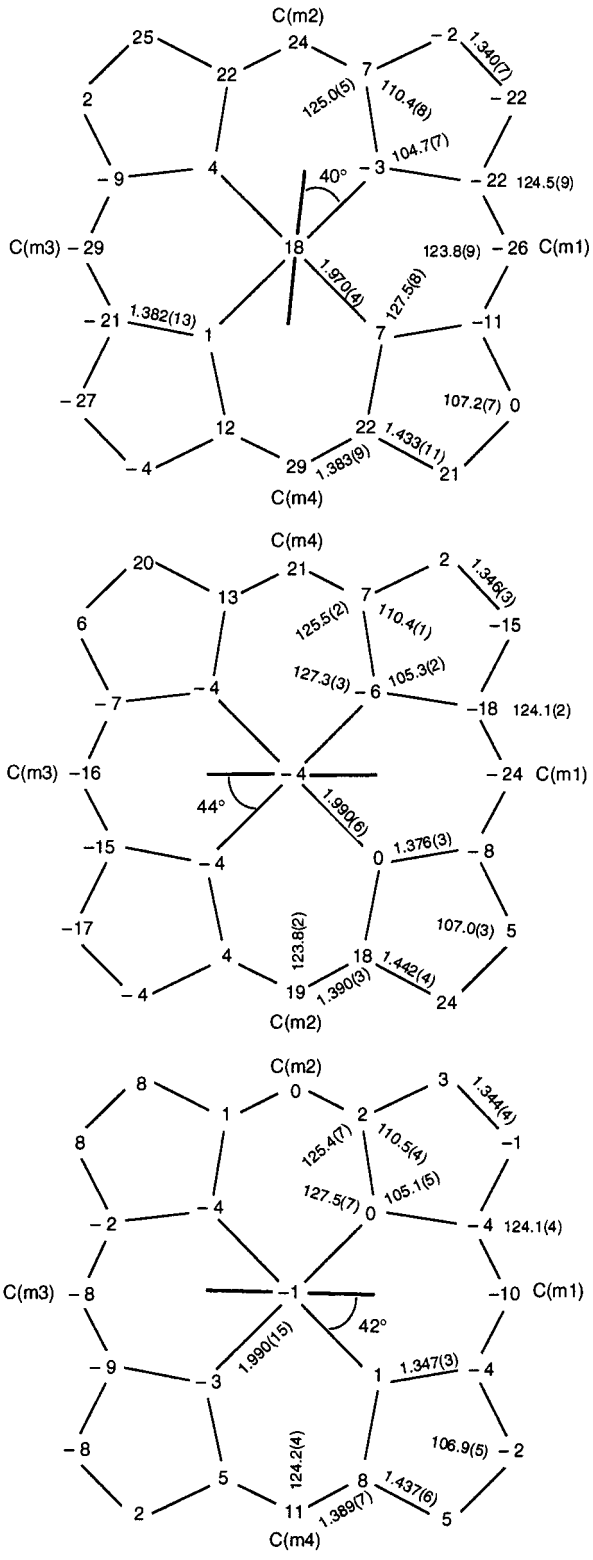

Figure 5. Formal diagrams of the porphinato core of $[Fe(TpivPP)(NO_2)]^-$ (top), $[Fe(TpivPP)(NO_2)(PMS)]^-$ (middle), and $[Fe(TpivPP)(NO_2)(Py)]^-$ (bottom). The view is from the nitrite side of the porphyrin (top view). Illustrated are the displacement of each unique atom from the mean plane of the 24-atom porphinato core in units of 0.01 Å. Positive values of displacements are toward the nitrite ion. The orientation of the nitrite ion is depicted with respect to the porphyrinato nitrogen atoms. Also displayed on the diagram are the averaged value of each type of bond distance and angle in the porphinato core.

to be unusually large, at 2.28 mm/s (Table 3). The quadrupole splitting is essentially temperature independent, with a value

Table 2. Bond Distances (Å) for (Nitro)iron Porphyrin Derivatives

complex	$Fe-N_p$[a]	$Fe-NO_2$	Fe−L	ref
$[Fe^{II}(TpivPP)(NO_2)]^-$	1.970(4)	1.849(6)		*b*
$[Fe^{II}(TpivPP)(NO_2)(PMS)]^-$	1.990(6)	1.937(3)	2.380(2)	*b*
$[Fe^{II}(TpivPP)(NO_2)(Py)]^-$	1.990(15)	1.951(5)	2.032(5)	*b*
$[Fe^{III}(TpivPP)(NO_2)(HIm)]$	1.974(2)	1.949(10)	2.037(10)	6
$[Fe^{III}(TpivPP)(NO_2)(Py)]$	1.985(3)	1.960(5)	2.093(5)	6
$[Fe^{III}(TpivPP)(NO_2)_2]^-$	1.992(1)	1.970(5)	2.001(6)	4
$[Fe^{III}(TpivPP)(NO_2)(SC_6HF_4)]^-$	1.980(7)	1.990(7)	2.277(2)	7
$[Fe^{III}(TpivPP)(NO_2)(NO)]$	1.996(4)	1.998(2)	1.671(2)	9
$[Fe^{II}(TpivPP)(NO_2)(NO)]^-$ (average of three values)	1.990(12)	2.075(5)	1.802(34)	8

[a] Average value.[23] [b] This work.

Table 3. Mössbauer Parameters for the Nitro Complexes and Related Derivatives[a]

complex	ΔE_Q (mm/s)	δ_{Fe} (mm/s)	*T* (K)	ref
Iron(II)				
$[Fe(TpivPP)(NO_2)]^-$	2.28	0.41	4.2	*c*
$[Fe(TpivPP)(NO_2)(PMS)]^-$	1.18	0.42	4.2	*c*
$[Fe(TpivPP)(NO_2)(Py)]^-$	0.93	0.41	4.2	*c*
$[Fe(TMP)(Py)_2]$	1.24	0.45	4.2	24
$[Fe(TPP)(Py)_2]$	1.15	0.40	77	25
$[Fe(OEP)(Py)_2]$	1.13	0.46	4.2	26
$[Fe(TpivPP)(1\text{-}MeIm)_2]$	1.02	0.46	4.2	27
$[Fe(TPP)(1\text{-}VinIm)_2]$	1.00	0.43	4.2	28
Iron(III)				
$[Fe(TPP)(NO_2)(NO)]$	1.37	0.02	293	9
	1.36	0.13	77	29
	1.36	0.13	4.2	9
$[Fe(T\ p\text{-}OCH_3PP)(NO_2)(NO)]$	1.43	0.04	293	9
$[Fe(TpivPP)(NO_2)_{in}(NO)_{out}]$	1.48	0.01	293	9
	1.43	0.09	4.2	9
$[Fe(TpivPP)(NO)_{in}(NO_2)_{out}]$	1.50	0.00	293	9
Iron(III)				
$[Fe(TpivPP)(NO_2)_2]^-$	2.1	0.25	4.2	6
$[Fe(TpivPP)(NO_2)(Py)]$	2.2	0.26	4.2	6
$[Fe(TpivPP)(NO_2)(SC_6HF_4)]^-$	2.12	0.22	293	7
	2.30	0.28	4.2	7
Iron(II)				
$[Fe(TpivPP)(NO_2)(NO)]^-$ (form 1)	1.78	0.22	200	8
$[Fe(TpivPP)(NO_2)(NO)]^-$ (form 2)	1.20	0.35	4.2	8
$[Fe(TPP)(THF)_2]$[b]	−2.75	0.96	4.2	30
$[Fe(TPP)(2\text{-}MeIm)]\cdot EtOH$[b]	2.28	0.93	4.2	27
$[Fe(TPP)(1,2\text{-}Me_2Im)]$[b]	−2.16	0.93	4.2	31

[a] Except as noted, all species are low spin. [b] High spin. [c] This work.

of $\Delta E_Q = 2.16$ mm/s at 190 K. We believe that the large observed Mössbauer quadrupole splitting for $[Fe(TpivPP)(NO_2)]^-$ results from a large rhombicity in the heme plane. When nitrite is the sole axial ligand, it must act as a very strong π acceptor. The dominance in the bonding of nitrite with respect to the heme plane then leads to a large difference in the energies of the d_{xz} and d_{yz} orbitals and a large quadrupole splitting. Such a large value of ΔE_Q for a low-spin iron(II) species has only been reported for oxygenated heme compounds such as oxyhemoglobin.[42] Two possibilities have been proposed to explain the unusually large quadrupole splitting in these species. First, the oxygenated heme was thought of as a superoxide ion ($S = {}^1/_2$) coordinated to a low-spin iron(III) ($S = {}^1/_2$), yielding a diamagnetic species due to resultant spin pairing.[43] The calculations of other investigators[44] suggested that the large ΔE_Q resulted from the asymmetric binding of dioxygen to iron, which caused a large rhombic distortion in the d_π orbitals. This latter

(42) Spartalian, K.; Lang, G. In *Applications of Mössbauer Spectroscopy;* Cohen, R. L., Ed.; Academic Press: New York, 1980; Vol. II, pp 249−279 and references therein.
(43) Weiss, J. J. *Nature (London)* **1964**, *202*, 83.
(44) Case, D. A.; Huynh, B. H.; Karplus, M. *J. Am. Chem. Soc.* **1979**, *101*, 4433.

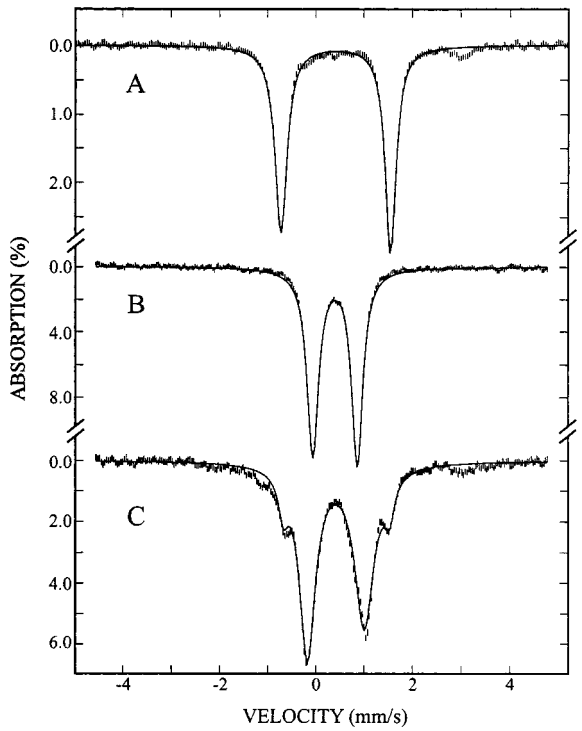

Figure 6. Mössbauer spectra of $[Fe(TpivPP)(NO_2)]^-$ (A), $[Fe(TpivPP)(NO_2)(Py)]^-$ (B), and $[Fe(TpivPP)(NO_2)(PMS)]^-$ (C) at 4.2 K in zero applied magnetic field. The solid lines are least-squares fits to the data, assuming two equal-area Lorentzian lines for each quadrupole doublet. The spectrum shown in (C) has a 15% contribution from the five-coordinate precursor. The parameters obtained are listed in Table 3.

explanation is also supported by more recent Mössbauer studies which show no evidence for a thermally accessible triplet excited state.[45] Furthermore, our observation of a large quadrupole splitting for $[Fe(TpivPP)(NO_2)]^-$ supports the idea of a large ligand-imposed rhombicity on the heme since an $Fe(III)-NO_2^{2-}$ formulation is highly improbable.

Mössbauer studies of $[Fe(TpivPP)(NO_2)]^-$ also confirm the low-spin-state description for the iron(II) center. Although the quadrupole splitting is found to be unusually large, the isomer shift of 0.41 mm/s is typical of low-spin iron(II) porphyrinates (see Table 3). The low-spin state is also confirmed by the Mössbauer data in a strong magnetic field, which shows that the magnetic field at the iron is equivalent to the applied field (i.e., $S = 0$).[46]

The data presented above are consistent with strong π-bonding between iron(II) and nitrite that is significantly stronger in the five-coordinate iron(II) system than in the six-coordinate iron(III) systems available for comparison. Similarly strong, or stronger, π-bonding is seen in the five-coordinate (porphinato)-iron nitrosyl complexes [Fe(Porph)(NO)] and $[Fe(Porph)(NO)]^+$. In these derivatives, the axial Fe−N(NO) distances are 1.717−1.734 Å for [Fe(Porph)(NO)][47−51] and 1.644 Å for $[Fe(Porph)(NO)]^+$.[52] The Fe−N(NO) distances in either class do not change upon addition of a neutral sixth ligand. The bond distance to the ligand trans to NO is, however, extremely long in derivatives formed from [Fe(Porph)(NO)][53,54] but normal in the derivatives formed from $[Fe(Porph)(NO)]^+$ species.[55]

To further investigate the bonding interactions of nitrite in iron(II) species, we set out to synthesize six-coordinate nitrite species. The mixed-ligand six-coordinate species $[Fe(TpivPP)(NO_2)(PMS)]^-$ and $[Fe(TpivPP)(NO_2)(Py)]^-$ are readily synthesized by the simple addition of a neutral sulfur- or nitrogen-donating ligand to five-coordinate $[Fe(TpivPP)(NO_2)]^-$ prepared in situ. The electronic spectra for the two species are shown in Figure 1, along with the electronic spectrum of $[Fe(TpivPP)(NO_2)]^-$. Obvious changes in the spectra result from the coordination of the sixth ligand. The Soret band strongly blue shifts from 444 nm in $[Fe(TpivPP)(NO_2)]^-$ to 432 and 429 nm for $[Fe(TpivPP)(NO_2)(PMS)]^-$ and $[Fe(TpivPP)(NO_2)(Py)]^-$, respectively. The intense visible bands in the six-coordinate complexes are also blue shifted by more than 30 nm from that of the five-coordinate precursor. The positions of these bands are typical of previously characterized six-coordinate low-spin iron(II) porphyrinates.[8,28,33] The spectra also show that the mixed-ligand species persist in solution in the presence of the neutral sixth ligand. We also note that the mixed-ligand species are significantly less oxygen sensitive in solution than $[Fe(TpivPP)(NO_2)]^-$.

The structures of six-coordinate $[Fe(TpivPP)(NO_2)(PMS)]^-$ and $[Fe(TpivPP)(NO_2)(Py)]^-$ are shown in Figures 3 and 4. The nitrite ligand is again N-bound and found inside the pocket formed by the pivalamide groups in both complexes. The orientation of the nitrite ligands with respect to the porphyrin cores is displayed in Figure 5. Again, the nitrite nearly bisects a N_p-Fe-N_p angle with values of 44 and 42° for the two species. The dihedral angle between the plane of the nitrite and the pyridine ligand plane is 81.4°. Upon coordination of the sixth ligand, the iron moves into the porphyrin plane and is actually displaced slightly toward the neutral ligands in both cases (see Figure 5). This figure also shows the modest S_4 ruffling of the porphyrin cores in all three derivatives. It should be noted that in the five-coordinate species the meso-carbon atoms along the nitrite direction are displaced on the nitro side of the plane, while the opposite is seen in the six-coordinate species. We take this to suggest that the ruffling is not related to the nitro ligand orientation.

The average $Fe-N_p$ bond length is 1.990(6) Å in $[Fe(TpivPP)(NO_2)(PMS)]^-$ and 1.990(15) Å in $[Fe(TpivPP)(NO_2)(Py)]^-$. These average equatorial bond lengths are the same as those found for the iron(II) six-coordinate species $[Fe(TpivPP)(NO_2)(NO)]^-$.[8] However, they are 0.02 Å longer than that of $[Fe(TpivPP)(NO_2)]^-$, which is quite short, at 1.970(4) Å. The bond length trans to nitrite in $[Fe(TpivPP)(NO_2)(PMS)]^-$ (Fe−S(PMS) = 2.380(2) Å) is slightly longer than the analogous bond length in related iron(II) derivatives. For example, in $[Fe(TPP)(THT)_2]$[56,57] there are two independent molecules in the unit cell, each with required inversion symmetry, and Fe−S(THT) is 2.338(1) Å in molecule 1 and 2.334(1) Å in molecule 2. The Fe−S distance in a related complex, [Fe(TPP)(SEt)(CO)], is 2.352 Å.[38] The bond length trans to nitrite in $[Fe(TpivPP)(NO_2)-$

(45) Boso, B.; Debrunner, P. G.; Wagner, G. C.; Inubushi, T. *Biochim. Biophys. Acta* **1984**, *791*, 244.
(46) The fit to the experimental data has been illustrated in Figure 2 of ref 12.
(47) Scheidt, W. R.; Frisse, M. E. *J. Am. Chem. Soc.* **1975**, *97*, 17.
(48) Bohle, D. S.; Hung, C.-H. *J. Am. Chem. Soc.* **1995**, *117*, 9584.
(49) Bohle, D. S.; Debrunner, P.; Fitzgerald, J.; Hansert, B.; Hung, C.-H.; Thompson, A. J. *J. Chem. Soc., Chem. Commun.* **1997**, 91.
(50) Ellison, M. K.; Scheidt, W. R. *J. Am. Chem. Soc.* **1997**, *119*, 7404.
(51) Scheidt, W. R.; Duval, H. F.; Neal, T. J.; Ellison, M. K. *J. Am. Chem. Soc.* **2000**, *122*, 4651.
(52) Scheidt, W. R.; Lee, Y. J.; Hatano, K. *J. Am. Chem. Soc.* **1984**, *106*, 3191.
(53) Scheidt, W. R.; Piciulo, P. L. *J. Am. Chem. Soc.* **1976**, *98*, 1913.
(54) Scheidt, W. R.; Brinegar, A. C.; Ferro, E. B.; Kirner, J. F. *J. Am. Chem. Soc.* **1977**, *99*, 7315.
(55) Ellison, M. K.; Scheidt, W. R. *J. Am. Chem. Soc.* **1999**, *121*, 5210.
(56) Mashiko, T.; Marchon, J.-C.; Musser, D. T.; Reed, C. A.; Kastner, M. E.; Scheidt, W. R. *J. Am. Chem. Soc.* **1979**, *101*, 3653.
(57) Mashiko, T.; Reed, C. A.; Kastner, M. E.; Haller, K. J.; Scheidt, W. R. *J. Am. Chem. Soc.* **1981**, *103*, 5758.

Table 4. Intramolecular Nonbonded Ligand-to-Porphyrin Distances[a]

complex	Fe−N(L)[b]	N(NO$_2$)···N$_p$[c]	O(NO$_2$)···N$_p$[d]	N(NO)···N$_p$[c]	O(NO)···N$_p$[e]	Δ[f]	O(NO$_2$)···C(a)[d]	O(NO)···C(a)	ref
[Fe(TpivPP)(NO$_2$)]$^-$	1.849(6)	2.76, 2.81(3)	2.98, 2.96	n.a.	n.a.	0.18[g]	3.22, 3.22	n.a.	12, *h*
[Fe(TpivPP)(NO$_2$)(PMS)]$^-$	1.937(3)	2.73, 2.77(3)	2.96, 2.89	n.a.	n.a.	0.04[i]	3.37, 3.32	n.a.	*h*
[Fe(TpivPP)(NO$_2$)(Py)]$^-$	1.951(5)	2.76, 2.79(2)	2.97, 2.96	n.a.	n.a.	0.01[j]	3.29, 3.40	n.a.	*h*
[Fe(TpivPP)(NO$_2$)(NO)]$^-$ [k]	1.792(8)	2.80, 2.83(2)	3.02, 3.03	2.64, 2.72(8)	3.04, 3.05	0.10[l]	3.26, 3.19	3.32	8
[Fe(TpivPP)(NO$_2$)(NO)]$^-$ [m]	1.774(8)	2.78, 2.83(5)	3.02, 3.00	2.65, 2.72(6)	3.00, 3.14	0.08[l]	3.35, 3.35	3.37	8
[Fe(TpivPP)(NO$_2$)(NO)]$^-$ [n]	1.840(6)	2.80, 2.82(1)	3.00, 2.99	2.68, 2.75(7)	2.95, 3.21	0.09[l]	3.42, 3.40	3.32	8
[Fe(OEP)(NO)] (*P*1̄)	1.7307(7)	n.a.	n.a.	2.69, 2.82(13)	3.13, 3.23	0.27[l]	n.a.	3.45	50
[Fe(TPP)(NO)(1-MeIm)]	1.743(4)	n.a.	n.a.	2.66, 2.70(4)	2.99, 3.31	0.07[l]	n.a.	3.61	53
[Fe(TPP)(NO)(4-MePip)][o]	1.721(10)	n.a.	n.a.	2.63, 2.70(6)	3.02, 3.04	0.09[l]	n.a.	3.38	54
[Fe(TPP)(NO)(4-MePip)][p]	1.740(7)	n.a.	n.a.	2.63, 2.72(8)	2.96, 3.29	0.11[l]	n.a.	3.52	54
[Co(OEP)(NO)]	1.8444(9)	n.a.	n.a.	2.78, 2.82(3)	2.97, 3.01	0.16[l]	n.a.	3.30	63
[Fe(OEP)(NO)]$^+$	1.644(3)	n.a.	n.a.	2.76, 2.78(1)	n.a.	0.29[l]	n.a.	n.a.	52
[Fe(TpivPP)(NO$_2$)(NO)]	1.671(2)	2.72, 2.75(3)	2.86, 2.87	2.57, 2.66(8)	n.a.	0.09[l]	3.27, 3.32	n.a.	9
[Fe(OEP)(NO)(1-MeIm)]$^+$	1.646(2)	n.a.	n.a.	2.59, 2.63(3)	n.a.	0.02[l]	n.a.	n.a.	55
[Fe(OEP)(NO)(Pz)]$^+$	1.627(2)	n.a.	n.a.	2.58, 2.63(4)	n.a.	0.01[l]	n.a.	n.a.	55

[a] Values in Å. [b] Shortest axial Fe−N distance is given. [c] Shortest distance listed first then average of four distances. [d] Shortest distance listed for each oxygen atom. [e] Values given are for the oxygen to the two closest porphyrin nitrogen atoms, and in cases of multiple oxygen atom positions due to disorder, the distance to the major oxygen atom position is given. [f] Displacement of the metal atom out of the 24-atom porphyrin plane toward the ligand specified in each case. [g] Toward nitrite. [h] This work. [i] Toward pentamethylene sulfide. [j] Toward pyridine. [k] Form 1, anion 1. [l] Toward nitrosyl. [m] Form 1, anion 2. [n] Form 2. [o] Unsolvated form. [p] Chloroform solvate.

(Py)]$^-$ (Fe−N(Py) = 2.032(5) Å) is comparable to the Fe−N(Py) bond lengths in a number of bis-pyridine iron(II) complexes,[24,58−61] where the axial Fe−N(Py) distance ranged from 1.996(2) to 2.039(1) Å. In the related CO complex, the Fe−N(Py) bond distance is longer, at 2.10(2) Å.[62]

Most notably in these (nitro)iron(II) species, upon coordination of a trans sixth ligand, the axial Fe−N(NO$_2$) bond length increases substantially. The Fe−N(NO$_2$) bond length has increased to 1.937(3) Å in [Fe(TpivPP)(NO$_2$)(PMS)]$^-$ and to 1.951(5) Å in [Fe(TpivPP)(NO$_2$)(Py)]$^-$ compared to the 1.849(6) Å value in [Fe(TpivPP)(NO$_2$)]$^-$. This ∼0.1-Å bond length increase must reflect distinct differences in the bonding interaction of nitrite in the five- and six-coordinate iron(II) species. The change in axial bond distances of nitrite is in distinct contrast to that of another nitrogen oxide ligand— nitrosyl (NO)—which acts as a strong π acceptor in both its five- and six-coordinate complexes. As noted earlier, the Fe−N(NO) length is effectively constant in both the five- and six-coordinate complexes in both of the two accessible oxidation states.

An increase in the Fe−N(NO$_2$) axial distance might be expected as a result of the ∼0.2-Å iron atom movement into the plane, which must lead to an increase in the nonbonded repulsions involving axial ligand atoms with the porphinato core if the axial distance remains unchanged. The nonbonded interactions are repulsions between the nitrogen and oxygen atoms of the axial ligand with atoms of the porphyrin core; those involving the coordinated nitrogen atom are more critical. The nonbonded distances involving the axial N and O atoms in the five- and six-coordinate iron(II) nitrite derivatives are tabulated in Table 4, along with the analogous N and O nonbonded distances in a number of five- and six-coordinate nitrosyl derivatives. It can be seen that, in the nitrosyl derivatives (both five- and six-coordinate), the nonbonded contacts are shorter than those seen in the nitrite complexes under discussion.

In all of these nitrogen oxide systems, the observed axial bond distance results from a balance of the (attractive) bonding interactions and the nonbonded repulsions. We believe that the data from the nitrosyl derivatives given in Table 4 suggest that the axial Fe−N(NO$_2$) distance in the six-coordinate iron(II) species could be as short as in the five-coordinate case, *were* the attractive interactions strong enough to demand it. This very strong attractive, coordination-number-invariant interaction is apparently the case in the nitrosyl derivatives. We interpret the data as follows. When nitrite is the sole axial ligand, as in [Fe(TpivPP)(NO$_2$)]$^-$, it acts as a very strong π acceptor. However, in the six-coordinate complexes with a neutral ligand trans to nitrite, the net π-accepting capabilities are apparently diminished, as seen in increased (≥0.10 Å) Fe−N(NO$_2$) bond lengths in the six-coordinate species. This is true even though the competing sixth ligands are not exceptional π-bonders. We suggest that the differences between NO$_2^-$ and NO bonding in iron(II) porphyrinates can be characterized as follows. NO is an obligatory π-bonding ligand, while nitrite can be described as a highly variable π-bonding ligand. The term "highly variable π-bonder" is meant to suggest that the nitrite ligand displays significantly different π-bonding in the various species it can form.

Mössbauer spectra provide additional evidence for this bonding interpretation. Upon coordination of the sixth ligand, the quadrupole splitting significantly decreases from the 2.28 mm/s in the five-coordinate complex to 1.18 ([Fe(TpivPP)(NO$_2$)(PMS)]$^-$) and 0.93 mm/s ([Fe(TpivPP)(NO$_2$)(Py)]$^-$) (Table 3). These ΔE_Q values are more typical of low-spin iron(II) porphyrinates.[27,28] The isomer shifts for all three (nitrite)iron(II) derivatives are similar and consistent with values for low-spin iron(II) porphyrinates. The large change in ΔE_Q upon the addition of a sixth ligand is interpreted as the result of a significant decrease in the π-bonding of nitrite with iron(II). This leads to decreased rhombicity of the d_{xz} and d_{yz} orbitals, which is manifested in the decreased ΔE_Q values.

Given the difference in the apparent π-bonding capabilities of the NO and NO$_2^-$ ligands, the previously described six-coordinate iron(II) species [Fe(TpivPP)(NO$_2$)(NO)]$^-$ [8] takes on renewed interest. We had previously described this complex as one in which the two nitrogen oxide axial ligands are expected to compete for π-bonding to iron(II). In fact, the nitrosyl ligand dominates the bonding, and the trans Fe−N(NO$_2$) bond length is a comparatively long 2.075(5) Å, an increase of over 0.2 Å compared to the iron nitrite bond length in [Fe(TpivPP)(NO$_2$)]$^-$. This very large change suggests that that there is little π-acceptor

(58) Li, N.; Petříček, V.; Coppens, P.; Landrum, J. *Acta Crystallogr., Sect. C* **1985**, *41*, 902.
(59) Li, N.; Coppens, P.; Landrum, J. *Inorg. Chem.* **1988**, *27*, 482.
(60) Grinstaff, M. W.; Hill, M. G.; Birnbaum, E. R.; Schaefer, W. P.; Labinger, J. A.; Gray, H. B. *Inorg. Chem.* **1995**, *34*, 4896.
(61) Balch, A. L.; Koerner, R.; Olmstead, M. M. *J. Chem. Soc., Chem. Commun.* **1995**, 873−874.
(62) Peng, S.-M.; Ibers, J. A. *J. Am. Chem. Soc.* **1976**, *98*, 8032.

character for the Fe−N(NO_2) bond in the mixed NO/NO_2^- complex. Again, the resulting bond distances are the net result of the combined attraction and nonbonded repulsions.

A comparison of the Fe−N(NO_2) bond lengths in the six-coordinate iron(II) and iron(III) species is given in Table 2. It is readily noted that there is a larger variation in Fe−N(NO_2) distance as a function of the (sixth) axial ligand in the iron(II) series than in the iron(III) series. From these comparisons, it appears that the nitrite to iron bonding shows a much larger variation in the iron(II) series; the component with the largest contribution to the variation must be the π donation of iron to nitrite. We also note that nitrite is always found to be N-bound in both the iron(II) and iron(III) porphyrinate complexes in contrast to ruthenium derivatives in which the nitrite is oxygen bound.[64]

The highly variable π-bonding nature of nitrite in the iron(II) porphyrinate system is made manifest by the relatively unusual circumstances of the availability of both square-pyramidal five-coordinate and pseudo-octahedral six-coordinate species with the same spin state and a common equatorial girdle of porphyrinate nitrogen atoms. Studies to show whether other π-acceptor ligands in iron porphyrinate systems behave similarly are in progress.

Summary. The molecular structure of the iron(II) low-spin five-coordinate complex [Fe(TpivPP)(NO_2)]$^-$ demonstrates that a complex with N-coordinated nitrite as the sole axial ligand can be synthesized. Structural and Mössbauer data show that nitrite is acting as a very strong π acceptor. Mössbauer data shows that the orientation of the d_π orbitals is determined by the axial nitrite ligand, which leads to a large rhombicity in the heme plane. Six-coordinate species can be synthesized by addition of neutral ligands to [Fe(TpivPP)(NO_2)]$^-$. Single-crystal structure determinations of two species show a substantial increase in Fe−N(NO_2) bond length upon coordination of the sixth ligand, suggesting a decrease in the π interaction between iron and nitrite. The observed axial bond distances result from a balance of the (attractive) bonding interactions and the nonbonded repulsions. This change in axial distances is in distinct contrast to the iron(II) and iron(III) nitrosyls, where the addition of a sixth ligand has no effect on Fe−N(NO). The Mössbauer parameters show that π-bonding to nitrite diminishes with six coordination, which is also consistent with the structural results.

Acknowledgment. We thank the National Institutes of Health for support of this research under Grant GM-38401 to W.R.S. and GM-58778 to B.H.H. Funds for the purchase of the FAST area detector diffractometer was provided through NIH Grant RR-06709 to the University of Notre Dame. We thank Dr. N. Ravi for assistance with the Mössbauer measurements. We are grateful to the reviewers, whose comments improved the manuscript.

Supporting Information Available: Tables S1−S18, listing the complete crystallographic details, atomic coordinates, bond distances and angles, anisotropic temperature factors, and fixed hydrogen atom positions for all three structures; Figures S1−S3, including ORTEP diagrams of the ordered potassium−Kryptofix counterions for all three structures as well as ORTEP diagrams of the disordered adventitious potassium−Kryptofix cation and nitrite/nitrate anion present in [Fe(TpivPP)(NO_2)(Py)]$^-$, and Figures S4 and S5, ORTEP diagrams showing the hydrogen-bonded water molecules present in the cell of [Fe(TpivPP)(NO_2)(Py)]$^-$; a written description of the disorder and the hydrogen-bonding is also included (PDF). This material is available free of charge via the Internet at http://pubs.acs.org.

JA000149A

(63) Ellison, M. K.; Scheidt, W. R. *Inorg. Chem.* **1998**, *37*, 382.

(64) (a) Kadish, K. M.; Adamian, V. A.; van Caemelbecke, E.; Tan, Z.; Tagliatesta, P.; Bianco, P.; Boshi, T.; Yi, G.-B.; Khan, M.; Richter-Addo; G. B. *Inorg. Chem.* **1996**, *35*, 1343. (b) Miranda, K. M.; Bu, X.; Lorković, I.; Ford, P. C. *Inorg. Chem.* **1997**, *36*, 4838.